Accepted Manuscript Synthesis, characterization and biological activity of new mixed ligand complexes of Zn(II) naproxen with nitrogen based ligands

ARTICLE *in* EUROPEAN JOURNAL OF MEDICINAL CHEMISTRY · OCTOBER 2014

Impact Factor: 3.45 · DOI: 10.1016/j.ejmech.2014.10.032

12 AUTHORS, INCLUDING:

Hijazi Abu Ali

Birzeit University

44 PUBLICATIONS **268** CITATIONS

SEE PROFILE

Mutaz Akkawi

Al-Quds University

36 PUBLICATIONS **318** CITATIONS

SEE PROFILE

Accepted Manuscript

Synthesis, characterization and biological activity of new mixed ligand complexes of Zn(II) naproxen with nitrogen based ligands

Hijazi Abu Ali, Hadeel Fares, Mohanad Darawsheh, Emilia Rappocciolo, Mutaz Akkawi, Suhair Jaber

PII: S0223-5234(14)00959-3

DOI: 10.1016/j.ejmech.2014.10.032

Reference: EJMECH 7439

To appear in: *European Journal of Medicinal Chemistry*

Received Date: 28 July 2014

Revised Date: 26 September 2014

Accepted Date: 12 October 2014

Please cite this article as: H.A. Ali, H. Fares, M. Darawsheh, E. Rappocciolo, M. Akkawi, S. Jaber, Synthesis, characterization and biological activity of new mixed ligand complexes of Zn(II) naproxen with nitrogen based ligands, European Journal of Medicinal Chemistry (2014), doi: 10.1016/j.ejmech.2014.10.032.

Synthesis, Characterization and Biological Activity of New Mixed Ligand Complexes of Zn(II) Naproxen with Nitrogen Based Ligands

Hijazi Abu Ali[a*#], Hadeel Fares[a#], Mohanad Darawsheh[a], Emilia Rappocciolo[b], Mutaz Akkawi[c] and Suhair Jaber[c]

Graphical Abstract

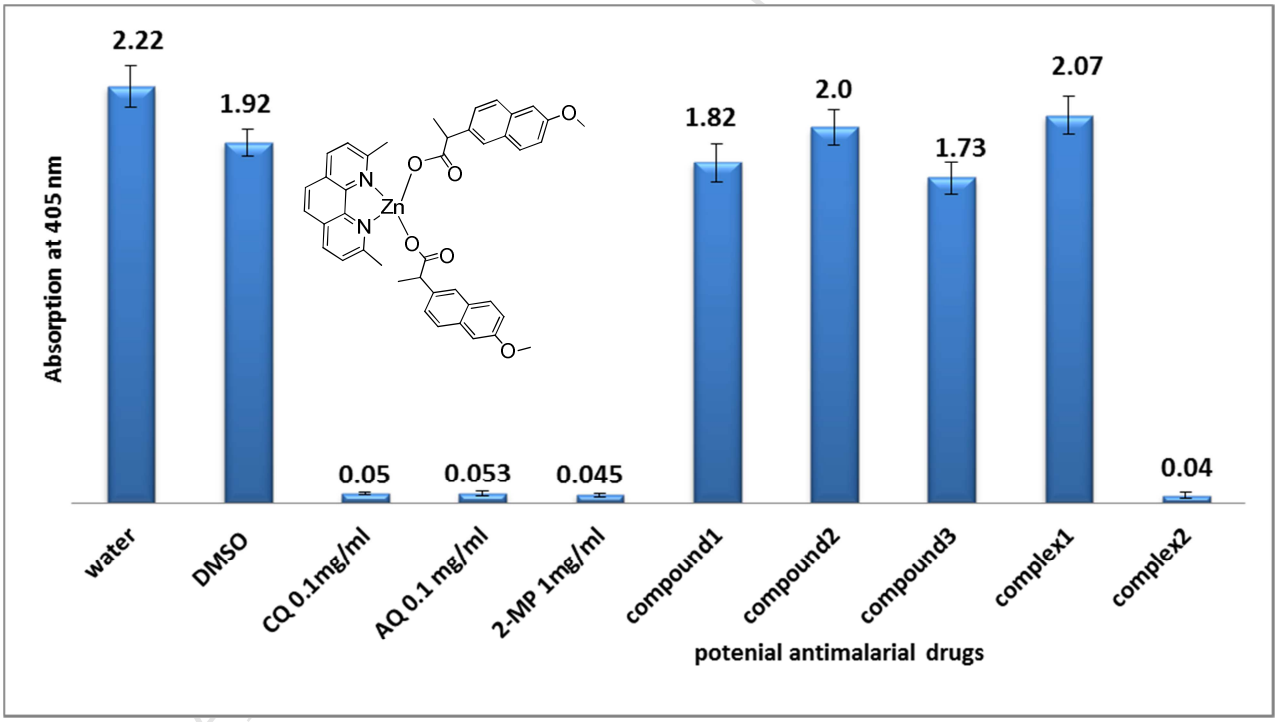

Synthesis, Characterization and Biological Activity of New Mixed Ligand Complexes of Zn(II) Naproxen with Nitrogen Based Ligands

Hijazi Abu Ali[a*#], Hadeel Fares[a#], Mohanad Darawsheh[a], Emilia Rappocciolo[b], Mutaz Akkawi[c] and Suhair Jaber[c]

[a]*Department of Chemistry, Birzeit University, West Bank, Palestine*

[b]*Department of Biology and Biochemistry, Birzeit University, West Bank, Palestine*

[c]*Department of Life Sciences , Al-Quds University , West Bank , Palestine*

[*]Corresponding author: Department of Chemistry, Birzeit University, P.O. Box 14, West Bank, Palestine

Tel: 00970 2 298 2146; Mobile: 00972 547 307 900; Fax: 00970 2 298 2084

e-mail: habuali@birzeit.edu, habuali1@yahoo.com

[#]Author contributions: These authors are contributed equally to this work

Abstract

A series of novel Zn(II) complexes $[Zn_2(nap)_4]$ **(1)**, $[Zn(nap)_2$1,10-phen**(2)**, $[Zn(nap)_2$2,9-dmphen] **(3)**, $[Zn(nap)_2(2\text{-ampy})_2]$ **(4)**, $[Zn(nap)_2(imid)_2]$ **(5)**, $[Zn(nap)_2(1,2\text{-dmimid})_2]$ **(6)** (nap = naproxen,1,10-phen = 1,10-phenanthroline, 2,9-dmphen = 2,9-dimethyl-1,10-phenanthroline, 2-ampy = 2-aminopyridine, imid = imidazole, 1,2-dmimid = 1,2-dimethyl imidazole) were synthesized and characterized using IR, UV-Vis, ^{1}H NMR, $^{13}C\{^{1}H\}$ NMR spectroscopy. The crystal structure of complex 3 was determined using single-crystal X-ray diffraction. In order to assess the effect of the metal ions on the anti-bacterial activity, complexes **1-6** have been screened *in vitro*, against (G^{+}) bacteria (*Staphylococcus aureus* and *Micrococcus luteus*) and (G^{-}) bacteria (*Klebsiella pneumoniae, Pseudomonas aeruginosa, Proteus mirabilis* and *Escherichia coli*) using the agar well diffusion method. Complex **2** was the only complex that showed antibacterial activity against *P. aeruginosa*, where the complexation of the parent ligand 1,10-phenathroline enhanced significantly the activity. All the complexes showed different activity against the different bacteria, and were compared with activity of the parent ligands. The complexes were tested also for their anti-malarial activity using two methods: a semi-quantitative micro-assay and a previously self-developed quantitative *in-vitro* method. Both were used to study the efficiency of these complexes in inhibiting the formation of the Malaria pigment. This is considered an important target of many known anti-malarial drugs such as Chloroquine and Amodaquine. Results showed that the efficiency of complex **3** in preventing the formation of β-Hematin was 75 %. The efficiency of Amodiaquine as a standard drug was reported to give 92.5.

Keywords: zinc(II) complexes, nitrogen-based ligands, naproxen, anti-bacterial activity, anti-malarial activity, β-hematin

1. Introduction

Zinc is one of the most important trace elements in the body and it is considered an essential element for many processes in living organisms [1-3]. Zinc ions exist primarily in the form of complexes with proteins and nucleic acids and participate in all aspects of intermediary metabolism, transmission and regulation of the expression of genetic information, storage, synthesis and action of peptide hormones and structural maintenance of chromatin, biomembranes and extracellular matrices [4]. Zinc ions possess some anti-bacterial effects, good thermal and color stability with low cost and little toxicity [5]. The growth of *Escherichia coli* is inhibited at high concentrations of zinc(II). However, low concentrations of zinc(II) have a promoting action on the growth of *E-coli* [6]. Zinc also can inhibit the growth of *Streptococcus faecalis, Klebsiella pneumoniae, Staphylococcus aureus* and some soil bacteria [7]. Many anti-bacterial drugs when chelated to the metal, show altered bioability and sometimes the chelated drug is more effective than the free ligand [8]. This is due to

the chelation of a bulky ligand to a metal cation which reduces the polarity of the ion and increases the lipophilicity of the metal complex, which can result in increased damage to bacterial cell walls and prohibit the transfer of zinc into the cell [9]. Malaria is one of the most prevalent parasitic diseases in the world. It is caused by different species of Plasmodium, Plasmodium vivax, Plasmodium falciparum, *Plasmodium malariae* and *Plasmodium ovale* of which *P.flaciparum* is the most virulent human malaria parasite. The parasite lives within human red blood cells and consumes over two thirds of the hemoglobin of the host cell. Digestion of hemoglobin by malaria parasite leads to the continuous liberation of free heme (Iron protoporphyrin IX) along with oxygen, causing formation of a ferric form of heme called ferri-protoporphyrin IX. This heme can lead to the killing of the parasite which has evolved a unique detoxification method of free heme through its conversion into a non-toxic, inert, insoluble, crystalline and black-brown pigment called homozoin [10-14]. β-Hematin crystals (Hemazoin) are made of dimer of hematin molecules that are oxygen coordinate bond links the central iron of one hematin to the oxygen of the carboxylate side-chain of the adjacent hematin [15]. Many clinically used antimalarial drugs such as chloroquine, amodaquine; mefloquine and 4-aminoquinoline are thought to act by inhibiting the formation of hemozoin in the food vacuole. This prevents the detoxification of the heme released in this compartment, and kills the parasite [16]. Chloroquine, a quinoline-ring drug, is widely used for malaria treatment. However, resistance to chloroquine has increased owing to extensive and uncontrolled use [17,18]. Chloroquine resistance is considered as major universal challenging problem and the need of new effective anti-malarial drugs is an urge. In this research both a semi-quantitative [19] and a quantitative screening methods for a new potential antimalarial drugs were used [20,21]. Naproxen [(+)-6-methoxy-α-methyl-2-naphthalene acetic acid], Fig.1 is a non-steroidal drug with antipyretic, anti-inflammatory and analgesic properties [22-24]. In addition, naproxen is used to relieve fever, pain and symptoms of arthritis, gout, bursitis and menstrual cramping. It acts as cyclooxygenase inhibitor that interferes with the COX-1 and COX-2 forms of that enzyme [25]. Some anti-inflammatory drugs are sodium salts of carboxylic acids; the Na metal can be replaced by transition metals to improve some of these drugs characteristics. Metal ion complexation with naproxen increases the transport of naproxen into the cells as supported by the fact that the transport of organic ligands into cells can be facilitated by the formation of metal complexes [24,26].

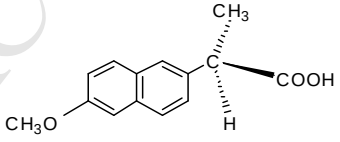

Fig. 1. Structural formula of D-naproxen.

Zinc complexes of aliphatic carboxylates such as formate, acetate, propionate and butyrate and aromatic carboxylates such as benzoate, 2-bromobenzoate 5-chlorosalicylate, 4-chlorosalicylate and salicylate with nitrogen based ligands have been synthesized and screened as bio-active compounds [1,6,27-38]. $Zn(naproxen)_2$

complex have been synthesized and characterized by IR, NMR and their anti-inflammatory studies were performed [24]. The interactions of this drug have been studied widely for copper with biologically active N-donor ligands such as 2,2-bipyridine, 1,10-phenanthroline and pyridine [22]. Other metal complexes of naproxen such as; the cobalt(II) complexes with naproxen in the presence of nitrogen–donor heterocyclic ligands (1,10-phenanthroline, 2,2-bipyridine and pyridine) have been synthesized and characterized with physiochemical and spectroscopic techniques [39]. The ligands 1,10-phenanthroline, 2,9-dimethyl-1,10-phenanthroline, 2-amino pyridine, imidazole and their derivatives, as well as many of their complexes, are exhibiting anti-bacterial [40-46], anti-viral [47,48], and anti-malarial [49-50], anti-fungal [51] and anti-tumor activities [49,52,53] depending on the nature of the ligand and the type of the metal ion. In this work, synthesis, characterization, antibacterial and antimalarial activity of novel mixed ligand complexes of Zn(II) naproxen with nitrogen based ligands i.e, 2,9-dimethyl-1,10-phenanthroline, 1,10-phenanthroline, 2-aminopyridine, imidazole and 1,2-dimethyl imidazole are reported. The crystal structure of complex **3** which showed a promised antimalarial activity was also determined.

2. Results and discussion

2.1 Synthesis of zinc complexes

[Zinc naproxen complex] **(1)** was prepared by reacting 1 eq of zinc chloride with 2 eq of sodium naproxen in water Scheme 1. The desired product was obtained as a white solid. Five mixed ligand zinc naproxen compounds have been prepared by the reaction of 1:2 molar ratio of complex **(1)** with the nitrogen donor ligands in acetone with stirring at ambient conditions Scheme 2. The physical properties of **1-6** are summarized in Table S1 (Appendix A. Supplementary Materials).

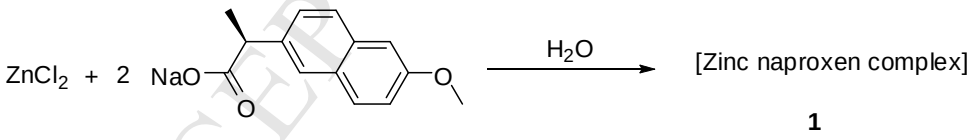

Scheme 1. Synthesis of complex 1.

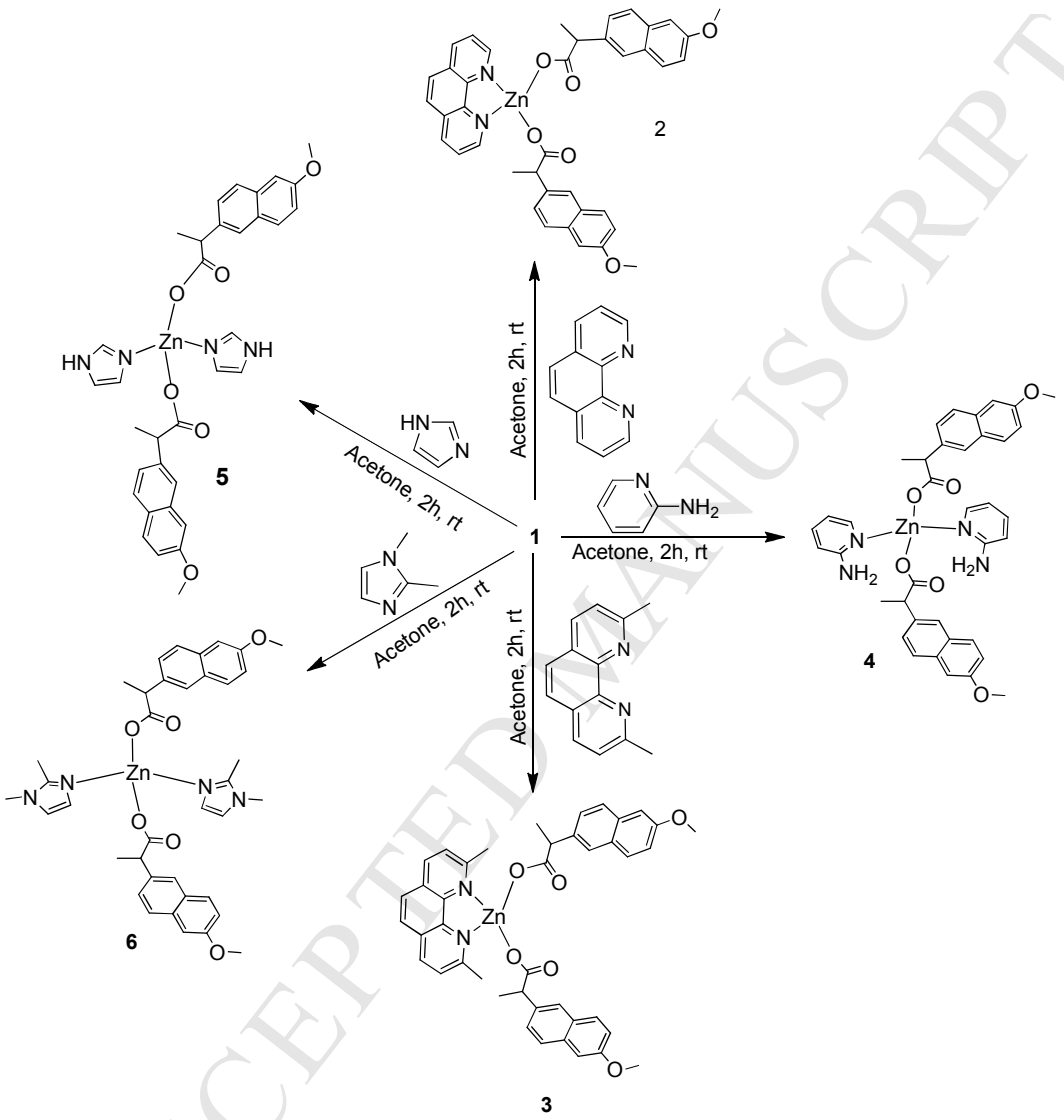

Scheme 2. Synthesis of complexes **2-6**

2.2 X-ray crystallographic study of complex 3

Suitable crystals for complex **3** were obtained by recrystallization from 1:1 mixture acetonitrile/chloroform and X-ray crystallographic analysis was determined. The crystal structure of complex **3** with the atomic labeling is illustrated in Fig. 2 and a summary of selected bond lengths and bond angles are given in Table S2.

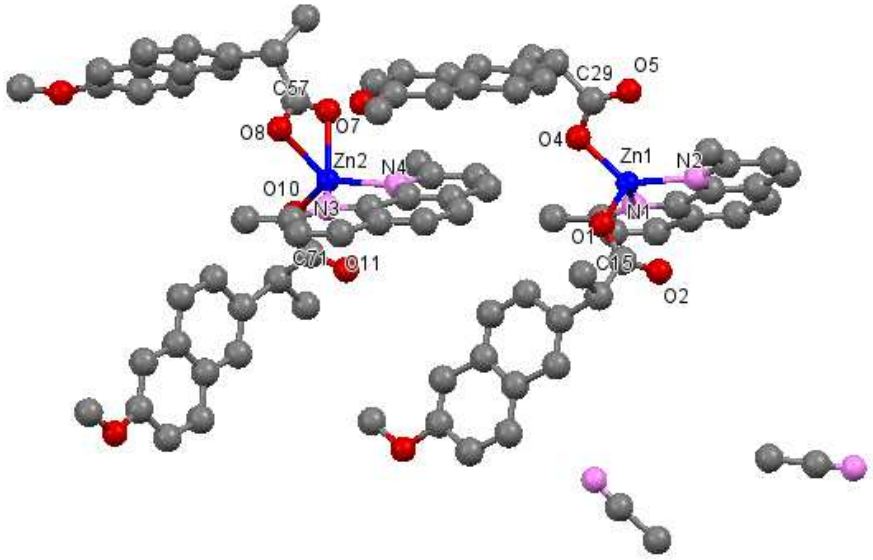

Fig. 2. View of the molecular structure of **3** showing the atom labeling scheme.

Complex **3** crystallized in the monoclinic space group *P2*(1) with four molecules in the unit cell and one acetonitrile molecule per each complex molecule. Two crystallographically inequivalent molecules of [Zn(nap)$_2$2,9-dmphen] exist in the asymmetrical unit, these two units are contacted by $\pi^{\cdots}\pi$ interaction between the aromatic group of naproxen in one molecule and the 2,9-dmphen of the other Fig. 3.

In the first asymmetrical molecule, zinc has a distorted tetrahedral ZnO_2N_2 chromophore; the Zn1 atom is coordinated to two monodentate oxygen atoms from naproxen ligands with Zn1-O1 and Zn1-O4 distances equal to 1.960 and 1.927 Å, respectively, this is in agreement with Zn-O bond distances in reported monodentate zinc benzoate complexes, zinc nitro benzoate complexes and 4-hydroxy benzoate complexes (1.96-2.20 Å) [54-56]. On the other hand, Zn1-O2 and Zn1-O5 non-bonded contacts are 2.927 and 2.792 Å, respectively. Bond angles around zinc are in agreement with tetrahedral angles (Table S2) with slight deviation that arises from the rigidity of the five-member ring that form with 2,9-dmphen.

In the second asymmetrical molecule of [Zn(nap)$_2$2,9-dmphen] with ZnO3N2 chromophore, using the geometrical parameter τ ($\tau = (\beta - \alpha)/60$, where β and α are the largest angles around the central atom) defined by Addison et al. [57]; the analysis of this complex gives a value of 0.11 which suggest a distorted square pyramidal

arrangement around Zn(II) atom. Here one of the naproxen coordinated in asymmetrical chelating bidentate coordination with Zn2-O7 and Zn2-O8 distances equal to 2.241 and 2.141 Å, respectively. The other naproxen is coordinated in monodentate mode, Zn2-O10 = 1.921 Å, and Zn2-O11 non-bonded contacts = 2.997 Å. The distorted tetragonal base plane is defined by the atoms O8, N4, N3 and O7. Deviation from regular tetragonal geometry is apparent from the observed binding angles, { N(3)-Zn(2)-O(8) = 91.39, N(3)-Zn(2)-O(7) = 137.59, N(4)-Zn(2)-O(7) = 97.05, N(4)-Zn(2)-O(8) = 130.98, O(7)-Zn(2)-O(8) =58.24} and the axial position are occupied by the O10. However, bond distances and angles within 2,9-dmphen and naproxen gave the expected values for such complexes.

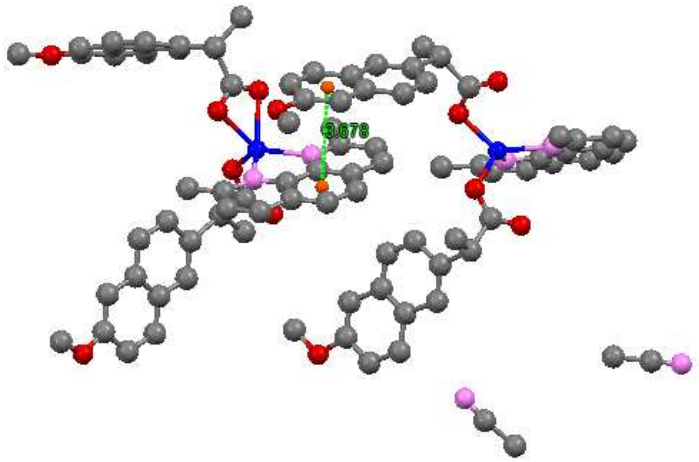

Fig. 3. π–π interactions of molecule **3**.

2.3 Infrared and UV-Vis spectra

Infrared spectral data of zinc naproxen complexes **1-6** in the 400-4000 cm^{-1} range as KBr disk are summarized in Tables S3-S6 (Appendix A Supplementary Materials). The IR frequencies for the sodium salts of naproxen and complex **1** are compared with previous literature data [24,26,58-60]. The asymmetric and symmetric $\upsilon(COO^-)$ stretching vibrations for sodium naproxen have been observed at 1540 and 1385 cm^{-1}, respectively, and the separation between them is $\Delta\upsilon(COO^-)$ = 155 cm^{-1}. In complex **1**, $\upsilon_{as}(COO^-)$ shifts to 1600 cm^{-1} and $\upsilon_s(COO^-)$ to 1390 cm^{-1} and $\Delta\upsilon(COO^-)$ = 210 cm^{-1} which is higher than $\Delta\upsilon(COO^-)$ of sodium naproxen [61]. Complex **1** may coordinated as *a monodentate mode* since [$\Delta_\nu(COO^-)_{\mathbf{1}}$ (210 cm^{-1}) >> $\Delta_\nu(COO^-)_{Na(nap)}$ (155 cm^{-1})] [62,63]. In accordance with literature data υ_{Zn-O} stretching vibrations for complexes **1-6** were found in the 412-578 cm^{-1} range [26,56].

The $\Delta\upsilon(COO^-)$ for complexes **2**, **3**, **4**, **5** and **6** were 215, 230, 216 196 and 229 cm^{-1}, respectively. This suggest monodentately coordinated carboxylate groups to the zinc atom (See Scheme 2), since $\Delta\upsilon(COO^-)$ of these complexes is higher than $\Delta\upsilon\ (COO^-)_{Na(nap)}$ (155 cm^{-1}) [64]. However, crystal structure of complex **3** showed three monodentate and one bidentate naproxen groups (See Fig. 2).

In the spectrum of complex **4** two bands were observed at 3335 and 3211 cm^{-1} which are attributed to the primary NH_2 group, υ_{as}(N-H) and υ_s(N-H), respectively.

Compared to the NH_2 stretching frequencies of 2-ampy ligand [ν_{as}(N-H) = 3447 and ν_s(N-H) = 3171 cm^{-1})], considerable shift caused by coordination to zinc was noticed.

In the IR spectrum of complex **6** showed one broad band at 3127 cm^{-1} which is attributed to the secondary NH bond stretching in the pyrimidine ring. Compared to the NH stretching frequencies of imidazole ligand (3125 cm^{-1}), a shift caused by coordination to zinc was also noticed. The IR frequencies of all zinc complexes, **2-6** were compared with their parent ligands and other zinc complexes [65-69].

UV-Visible absorption of all zinc complexes, **1-6** in the 200-700 nm range were carried out and compared with their parent ligands in which only small shift caused by coordination to zinc was observed Table 1.

The absorption bands of these metal complexes (in the 200-350 nm range) may be attributed to π-π* and *n*-π* transitions, however, metal to ligand charge transfer transition may occur in this range although it was difficult to assign any of them due to overlap with ligand transitions. Moreover, the *d* orbital in the zinc(II) atom is completely filled; so no *d-d* transition bands have been detected in all zinc complexes.

Table 1

UV-Vis data of complexes **1-6**

Complex	λ_{max} (nm)	ε_{max} ($L.mol^{-1}.cm^{-1}$)
1	264, 274, 333	962, 923, 270
2	233,271, 292,318,333	17903, 4902, 1349, 419, 455
3	274,298,319,333	3400,1531,571,560
4	265,275, 320, 333	1418, 1626, 520, 500
5	264, 274,320, 334	1064, 1148, 470, 491
6	264, 274,320, 335	632, 705, 350, 400

2.4 ^{1}H NMR and ^{13}C{^{1}H} NMR results

The ^{1}H and ^{13}C{^{1}H} NMR spectral data for **1-6**, naproxen and the parent N-donor ligands are reported in Tables S6-S11 (Appendix A. Supplementary Materials) . The results are in agreement with the proposed structures as shown in Scheme 2. The ^{1}H NMR and ^{13}C{^{1}H} chemical shifts of naproxen and the N-donor ligands were found in the expected positions of free ligands with a shift due to the coordination with metal. The value of δ ^{13}C chemical shift of the (CH_3) of naproxen for **1-6** and the free naproxen are summarized in Table 2. This carbon is chosen for comparison because it is close to the coordination site (COO^-) on one hand; and it is less affected by other external conditions on the other hand. This carbon exhibited downfield chemical shift in the range of 0.51-1.29 ppm compared to the free naproxen ligand value; which resulted from complex formation. The integration ratios of the ^{1}H NMR signals of **2-6** are in agreement with the proposed structure as shown in Scheme 2. The proposed structures were also determined by comparison with similar published data [22].

Table 2

$^{13}C\{^{1}H\}$ NMR spectral data of the CH_3 carbon of naproxen for **1-6**.*

Compound	δ (CH_3)
1	19.59
2	19.58
3	19.75
4	19.60
5	20.36
6	20.36
Naproxen	19.07

*ppm downfield relative to TMS as internal standard ($CDCl_3$).

2.5 *In vitro* anti-bacterial activity results

The solution stability of the complexes were checked by repeated ^{1}H and $^{13}C\{^{1}H\}$ NMR measurements in DMSO and $CDCl_3$ solvents and they proved high solution stability. Zinc naproxen complexes **1-6** were tested for their anti-bacterial activity against G+ bacteria *(S. aureus* and *M. luteus)* and G- bacteria *(K. pneumoniae, P. mirabilis, P. aeruginosa* and *E. coli).* The anti-bacterial screening data were summarized in Table 3 using DMSO as a negative control while Erythromycin and Gentamycin used as positive controls. Sodium naproxen and Zn(II) as chloride did not show any significant activity at the same concentration, but Erythromycin as positive control showed high anti-bacterial activity against all tested bacterial species (except *P. aeruginosa*) with inhibition zone 17-43 mm, Gentamycin as positive control showed high anti-bacterial activity against all tested bacterial species with inhibition zone of 23-33 mm.

Table 3

Anti-bacterial activity data of complexes **1-6** in (mm)/8.5 mmol/L.

	G^{+}bacteria		G^{-}bacteria			
Complex	*M. luteus*	*S. aureus*	*P. aeruginosa*	*E. Coli*	*K. pneumonia*	*P. mirabilis*
(1)	----------	----------	----------	10.0 ± 1.0	10.0 ± 1.0	8.0 ± 0.6
(2)	16.0 ± 2.1	16.0 ± 1.1	19.0 ± 1.1	20.0 ± 2.1	20.0 ± 2.5	21.0 ± 1.0
(3)	20.0 ± 1.5	20.0 ± 1.0	----------	7.7 ± 1.2	11.0 ± 1.2	----------
(4)	12.3 ± 1.2	12.3 ± 0.6	----------	----------	----------	----------
(5)	----------	----------	----------	9.7 ± 0.6	9.7 ± 0.6	----------
(6)	8.7 ± 0.6	8.3 ± 1.2	----------	----------	----------	----------
Naproxen	----------	----------	----------	----------	----------	----------
$ZnCl_2$	----------	----------	----------	----------	----------	----------
Erythromycin	39.0	43.0	----------	18.0	21.0	17.0
Gentamycin	33.0	27.0	23.0	28.0	32.0	28.0

Complex **1** showed low anti-bacterial activity with inhibition zone 8-10 mm for *P. mirabilis, E. coli* and *K. pneumonia*. Complex **2** showed high anti-bacterial activity

against all tested bacterial species with inhibition zone 16-21 mm. Although complex **3** showed high anti-bacterial activity against G^+-bacterial with inhibition zone around 20 mm, it showed low anti-bacterial activity against G^--bacteria with inhibition zone 7.7-11 mm. Complex **4** showed intermediate anti-bacterial activity only against G^+-bacteria with inhibition zone around 12 mm. Complexes **5** and **6** showed low anti-bacterial activity against *E. coli* and *K. pneumonia* (with inhibition zone around 9.7 mm) and *S. aureus* and *M. luteus* (with inhibition zone around 8.5 mm), respectively. Due to their higher anti-bacterial activity, complexes **2**, **3** and **4** were compared with their parent nitrogen donor ligands against all tested bacterial species to determine the effect of the complexation on anti-bacterial activity. Different dilutions of these complexes and their parent ligands in DMSO in the concentration range 8.50-2.12 mmol/L were prepared using the same procedure. In this part the complexes and their parent ligands were tested in the same plate and in the same conditions to determine the MIC. The anti-bacterial results were summarized in Table 4.

Table 4

In-vitro anti-bacterial activity data at different concentrations and the MIC values of complexes **2, 3, 4** and their parent ligands.

	M. luteus	***S. aureus***	***P. Aeruginosa***	***E. Coli***	***K. pneumoniae***	***P. mirabilis***
Diameter of inhibition zone of Complex **(2)** (mm)						
8.50 mmol/L	16.0	16.0	19.0	20.0	20.0	21.0
4.25 mmol/L	13.0	14.0	14.0	16.0	17.0	16.0
2.12 mmol/L	9.0	10.0	12.0	14.0	14.0	14.0
MIC (mmol/L)	2.12	1.06	2.12	0.265	1.06	1.06
Diameter of inhibition zone of 1,10-phenanthroline ligand (mm)						
8.50 mmol/L	29.0	30.0	8.0	27.0	25.0	30.0
4.25 mmol/L	25.0	24.0	7.0	23.0	20.0	24.0
2.12 mmol/L	17.0	17.0	----------	18.0	15.0	17.0
MIC (mmol/L)	0.531	1.06	4.25	0.531	0.531	0.531
Diameter of inhibition zone of Complex (**3**) (mm)						
8.50 mmol/L	20.0	20.0	-------	7.7	11.0	--------
4.25 mmol/L	18.0	18.0	-------	7.7	11.0	--------
2.12 mmol/L	17.0	16.0	-------	7.0	10.0	-------
MIC (mmol/L)	0.531	0.265	> 8.50	1.06	0.265	> 8.50
Diameter of inhibition zone of 2,9-dimethyl-1,10-phenanthroline ligand (mm)						
8.50 mmol/L	21.0	24.0	--------	--------	8.0	-------
4.25 mmol/L	19.0	21.0	--------	--------	7.0	-------
2.12 mmol/L	12.0	19.0	--------	--------	------	-------
MIC (mmol/L)	2.12	0.265	> 8.50	> 8.50	4.25	> 8.50
Diameter of inhibition zone of Complex (**4**)* (mm)						
8.50 mmol/L	12.0	12.0	----------	---------	----------	----------
4.25 mmol/L	10.0	10.0	----------	----------	---------	----------
2.12 mmol/L	9.0	8.0	----------	----------	----------	----------
MIC (mmol/L)	0.531	1.06	>8.50	>8.50	>8.50	>8.50

*The parent ligand of this complex 2-aminopyridine did not show any biological activity on this concentration range.

The results presented in Table 4 showed that the anti-bacterial activity of 1,10-phenanthroline ligand showed higher anti-bacterial activity than complex **2** against all tested bacterial species (except *P. aeruginosa*) where the complexation of the ligand 1,10-phenanthroline with zinc naproxen decreased the anti-bacterial activity. In the case of *P. aeruginosa,* complex **2** exhibit very good activity and notably higher than the parent ligands. Complex **2** was the only structure which showed anti-bacterial activity against *P. aeruginosa.*

Complex **3** showed higher anti-bacterial activity against G^+-bacteria than G^--bacteria. Also this complex showed higher anti-bacterial activity against G^--bacteria compared to 2,9-dimethyl-1,10-phenanthroline ligand. On the other hand, the activity of complex **2** and the parent ligand are similar against the G^+-bacteria. This difference could be explained by the different cell wall structure of G^+-bacteria and G^-- bacteria. It is possible that the enhancement of lipophilicity of complex **2** plays a role in the increased activity against G^-- bacteria.

Complex **4** showed anti-bacterial activities only against G^+ bacteria. 2-Aminopyridine ligand did not show anti-bacterial activity against all tested bacterial species. The complexation of the ligand 2-aminopyridine with zinc naproxen increased the anti-bacterial activity against G^+ bacteria.

2.6 Anti-malarial activity

2.6.1 Semi-quantitative method

Two different zinc naproxen complexes **2** and **3**, and their parent phenanthroline derivative ligands were all evaluated for their inhibitory effect on *in-vitro* beta-hematin formation. Results of the semi-quantitative method are shown in Fig. 4 and Fig. 5 (complexes **1**, **2**, **4**, **5** and **6** did not show any significant inhibitory effect on *in-vitro* beta-hematin formation; complex **2** was used as a comparison on figure **3** because of the similarity in structure with the active complex **3**).

As shown in Fig. 4, complex **3** with an absorbance value of 0.04 (at a concentration of 1 mg/ml) was the only one of these four compounds with a potential anti-malarial activity when compared to the standard drugs (at a concentration of 0.1 mg/ml). The efficiency of the drug used is inversely proportional to the absorption, low absorption indicates higher efficiency and vice versa. It is important to mention that each result is the average of 26 individual experiments. It is obvious that complex **3** needs more investigation and the test was repeated using lower concentrations of this complex. Different dilutions of complex **3** were made and the results are summarized in Fig. 5. Complex **3** with the range of concentrations between 1-0.6 mg/ml showed a good inhibition activity on the formation of β-hematin, also no inhibition was noticed at 0.5 mg/ml.

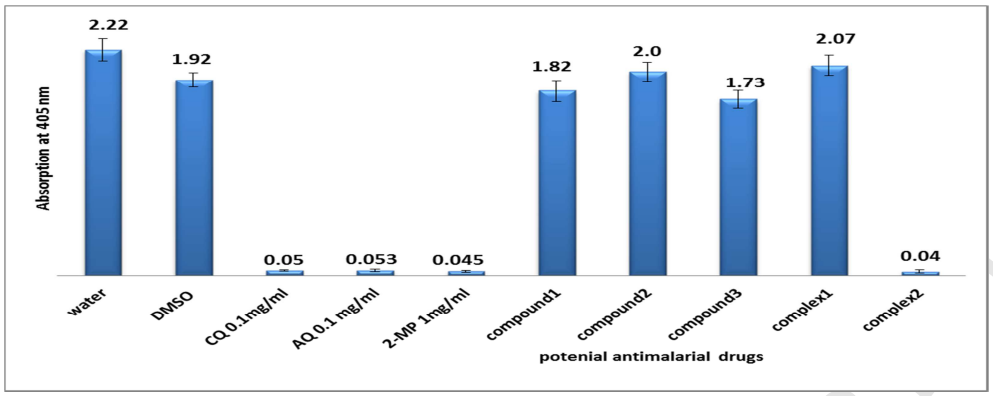

Fig. 4. Column diagram representing Semi-Quantitative test results of potential anti-malarial drugs, (compound 1): Zn naproxen complex, (compound 2): 1,10-phenanthroline, (compound 3): 2,9 dimethyl-1,10-phenanthroline (complex 1): $Zn(nap)_2$1,10-phen and (complex 2): $Zn(nap)_2$-2,9 dmphen ,all at concentration 1mg/ml dissolved in DMSO, compared to Chloroquine (CQ) Amodiaquine (AQ) and 2-mercaptopyramidine (2-MP) as positive controls, while water and DMSO were used as negative controls, absorption is inversely proportional to drugs efficiency, the lower the absorption is, the drug is considered to be more efficient.

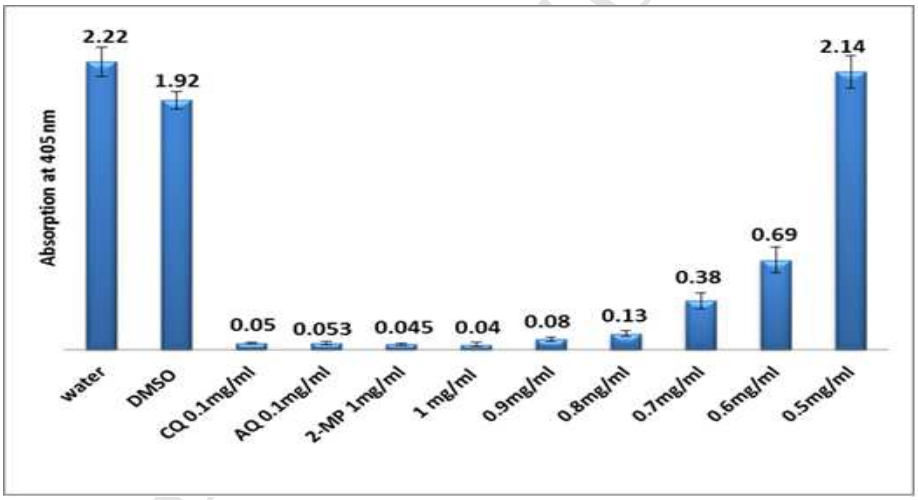

Fig. 5. Column diagram representing the Semi-Quantitative test results of potential anti-malarial drug $Zn(nap)_2$-2,9-dimethyl-1,10 phenanthroline dissolved in DMSO, compared to Chloroquine, Amidoquine and 2-Mercaptopyrimidine as positive controls. while water and DMSO used as negative controls, showing the absorption values of dissolved β-Hematin (alkaline hematin) at 405 nm using ELISA reader, absorption is inversely proportional to drugs efficiency, the lower the absorption is, the drug is considered to be more efficient.

2.6.2 Quantitative method:

According to method of use, the result of complex compared to DMSO (as negative control) and Amodiaquine (AQ as positive control) in terms of β-Hematin formation is shown in Fig. 6. Comparison in terms of drug efficiency is seen in Fig. 7.

Fig. 6 represents the percentage yield of β-Hematin formation. Interestingly, the percentage yield of β-hematin formation in the presence of complex **3** was 25% and that of AQ was 7.5%, both at concentration 0.4 mM comparing to the negative control which was 87.5%.

Comparison in terms of efficiency of the complex under investigation as anti-malarial drug is shown in Fig. 7. It is obvious that complex **3** has a considerable anti-malarial

activity in inhibiting β-hematin formation with efficiency 75%, when compared to AQ 92.5%, and DMSO 12.5%.

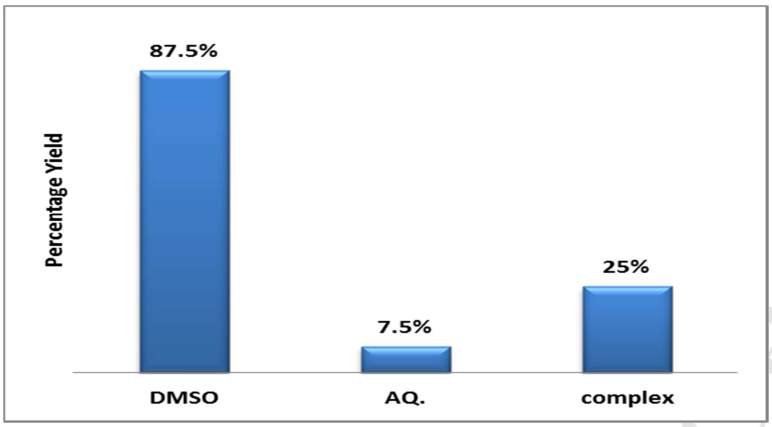

Fig. 6. Column diagram representing the percentage yields of complex: $Zn(nap)_2$-2,9-dmphen as potential anti-malarial drug, compared to Amidoquine and DMSO at 0.4 mM. Yields are inversely proportional to drugs efficiency, the lower the yield is, the drug is considered to be more efficient.

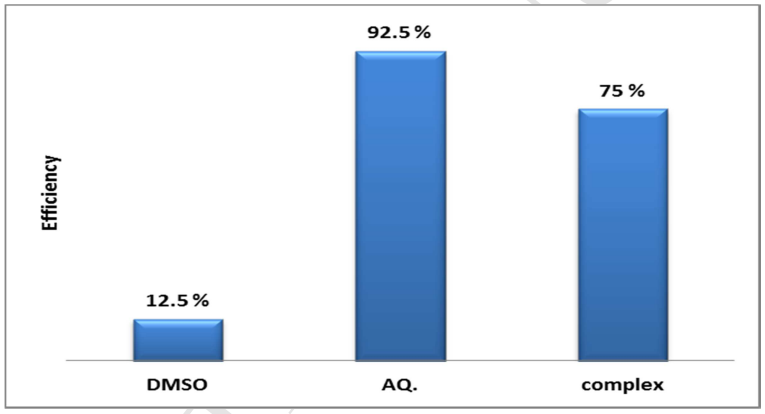

Fig. 7. Column diagram representing the efficiencies of potential anti-malarial drug, $Zn(nap)_2$-2,9-dmphen, compared to Amidoquine, all at a concentration of 0.4 mM.

This inhibition activity of β-hematin may be due to the interactions between complex **3** and ferri-heme; which inhibited the formation of β-hematin *in vitro*. Forces involved in stability of this interactions may involve π-π stacking forces of the phenanthroline ring over the porphyrin, hydrogen bonding interaction between naproxen oxygen atoms and propanoic acid of the ferri-heme and coordination bond between zinc(II) and the N-donor groups of the heme [70].

Complex **(2)** (see Fig. 3) did not show any considerable activity although it is similar to complex **3**. These two complexes are only different in the methyl groups in the 1 and 9 positions of the phenanthroline in complex **3**. The additional methyl groups of the 2,9-dimethyl-1,10-phenanthroline may form electrostatic interaction with ferri-heme may be play a major rule in stabilizing the interaction with ferri-heme. The mechanism of inhibition is thought to be through the formation of a complex between complex **3** and ferriheme which prevent the formation of β-hematin.

3. Experimental

3.1 Instruments

Infrared (IR) absorption spectra were recorded using a Varian 600 FT-IR spectrometer in the region of 400-4000 cm^{-1} using KBr pellet technique. ^{1}H and $^{13}C\{^{1}H\}$ NMR spectra were recorded in $CDCl_3$ and DMSO (d^6) as solvents with a Varian Unity spectrometer (300 and 75 Hz) for ^{1}H and $^{13}C\{^{1}H\}$ nucleus, respectively. UV-Vis measurements were recorded on a Hewlett Packard 8453 photo diode-array spectrometer in the 200–800 nm region using DMSO, $CHCl_3$, and CH_3OH as solvents. Melting points were determined in capillary tube with EZ-melt apparatus and are uncorrected.

3.2 Materials

The starting materials used in the present work were purchased from Sigma-Aldrich with high purity and were used without further purification. Solvents were also purchased from commercial sources. Pure cultures of *Micrococcus luteus, Staphylococcus aureus, Pseudomonas aeruginosa, Escherichia coli, Klebsiella pneumoniae and Proteus mirabilis* were obtained from the Biology and Biochemistry Department at Birzeit University.

3.3 Synthesis

3.3.1 Synthesis of [zinc naproxen complex] (1)

Zinc naproxen complex was prepared by reacting 1 eq of zinc chloride with 2 eq of sodium naproxen in 70 ml H_2O solvent at room temperature. The complex thus formed was filtered, washed with water and air dried. Zinc naproxen was also previously prepared as shown in the literature [24-26].The complex is soluble in acetone, dichloromethane, methanol, ethanol and acetonitrile. **(1)**: (86%) yield**,** m.p. (228-233) ^{o}C; ^{1}H NMR ($CDCl_3$): δ = 1.39 (d, 3H, CH_3), 3.70 (bs, 1H, CH), 3.90 (s, 3H, OCH_3), 7.00 (bs, 1H, CH), 7.08 (d, 1H, CH, ^{3}J = 8.4 Hz), 7.42 (bs, 1H, CH), 7.54 (s, 1H, CH), 7.58 (d, 1H, CH), 7.61 (d, 1H, CH); $^{13}C\{^{1}H\}$ NMR ($CDCl_3$): δ = 19.59 (CH_3), 48.37 (**C**H-CH_3), 55.44 (O-CH_3), 105.70 (CH), 118.82 (CH), 125.88 (CH), 126.87 (CH), 127.17 (CH), 129.26 (CH), 133.51 (CH), 157.44 (**C**-OCH_3), 181 (C=O); IR (cm^{-1}, KBr): 3080, 2955, 1696, 1630, 1600, 1485, 1455, 1390, 1370, 1260, 1210, 1160, 1027, 974, 927, 811, 744, 615, 591; UV-Vis, ($CHCl_3$), λ (nm): 264, 274, 333.

3.3.2 Synthesis of [$Zn(nap)_2$1,10-phen] (2)

1,10-Phenanthroline (0.45 g, 2.3 mmol) was dissolved in 30 ml acetone and added drop-wise to a stirred acetone solution of **(1)** (0.6 g, 1.1 mmol). The solution was stirred for 2 h and a white solid was formed which was then filtered and air dried. The compound is soluble in dichloromethane and methanol.

[Zn(nap)$_2$1,10-phen] **(2)** :(80%) yield, m.p. (220-230) ^{o}C; ^{1}H NMR ($CDCl_3$): δ = 1.52 (d, 3H, CH_3, $^3J_{H-H}$ = 6.9 Hz), 3.87 (bs, 4H, CH, OCH_3), 7.02 (d, 1H, CH, $^3J_{H-H}$ = 3 Hz), 7.06 (d, 1H, CH, $^3J_{H-H}$ = 1.5 Hz), 7.40 (d, 2H, CH, $^3J_{H-H}$ = 8.1 Hz), 7.49 (d, 1H, CH, $^3J_{H-H}$ = 8.7 Hz), 7.52 (d, 2H, 2CH), 7.60 (bs, 2H, CH_{Phen}), 7.68 (t, 2H, CH_{Phen}, $^3J_{H-H}$ = 7.8 Hz), 7.81 (bs, 2H, CH_{Phen}), 8.53 (d, 2H, CH_{Phen}); ^{13}C{^{1}H} NMR ($CDCl_3$): δ = 19.58 (CH_3), 46.67 (**C**H-CH_3), 55.49 (O-CH_3), 105.69 (CH), 118.59 (CH), 120.96 ($2CH_{Phen}$), 125.86 (CH), 126.74 (CH), 127.34 (CH), 129.12 (CH), 129.44 ($2CH_{Phen}$), 133.48 (CH), 138.68 ($2CH_{Phen}$), 139.91 ($2CH_{Phen}$), 149.64 ($2CH_{Phen}$), 157.38 (**C**-OCH_3), (C=O) was undetectable; IR (cm^{-1}, KBr): 3058, 2969, 2931, 2837, 1603, 1522, 1483, 1458, 1430, 1388, 1262, 1159, 1121, 1061, 1029, 960, 927, 852, 824, 777, 726, 697, 543, 475, 429; UV-Vis, (MeOH), λ (nm): 233, 271, 292, 319, 333.

3.3.3 Synthesis of [Zn(nap)$_2$2,9-dmphen] (3)

Same procedure was followed as in complex **2** except with 2,9-Dimethyl-1,10-phenanthroline (0.49 g, 2.3 mmol) and complex **(1)** (0.67 g, 1.15 mmol). Suitable crystals for X-ray structural analysis were obtained by recrystallization from 1:1 mixture of acetonitrile and chloroform. The compound is soluble in chloroform, acetonitrile and acetone.

[Zn(nap)$_2$2,9-dmphen] **(3)**: (72%) yield, m.p. (209-213) ^{o}C; ^{1}H NMR ($CDCl_3$): δ = 1.49 (d, 3H, CH_3, $^3J_{H-H}$ = 7.2 Hz), 2.74 (s, 6H, CH_{3Phen}), 3.86 (q, 1H, CH), 3.89 (s, 3H, OCH_3), 7.03 (bs, 1H, CH), 7.06 (d, 1H, CH, $^3J_{H-H}$ = 2.7 Hz), 7.40 (d, 2H, CH_{Phen}, $^3J_{H-H}$ = 2.7 Hz), 7.43 (d, 1H, CH), 7.51 (d, 2H, CH_{nap}, $^3J_{H-H}$ = 8.7 Hz), 7.59 (bs, 1H, CH), 7.69 (d, 2H, CH_{Phen}, $^3J_{H-H}$ = 3.9 Hz), 8.17 (d, 2H, CH_{Phen}, $^3J_{H-H}$ = 8.4 Hz); ^{13}C{^{1}H} NMR ($CDCl_3$): δ = 19.75 (CH_3), 24.81 ($2CH_{3Phen}$), 47.06 (**C**H-CH_3), 55.48 (O-CH_3), 105.70 (CH), 118.49 (CH), 125.70 ($2CH_{Phen}$), 125.81 (CH), 126.36 ($2CH_{Phen}$), 126.61 (CH), 127.12 (CH), 127.39 ($2C_{phen}$), 129.29 (CH), 132.12 ($2CH_{Phen}$), 133.40 (CH), 139.11 ($2CH_{Phen}$), 157.29 (**C**-OCH_3), 160.76 ($2CH_{Phen}$), 181.87 (C=O); IR (cm^{-1}, KBr): 3056, 2964, 2930, 1605, 1505, 1453, 1375, 1270, 1212, 1156, 1121, 1033, 927, 852, 813, 782, 750, 683, 661, 549, 475, 416; UV-Vis, (DMSO), λ (nm): 274, 298, 319, 333.

3.3.4 Synthesis of [Zn(nap)$_2$(2-ampy)$_2$] (4)

2-Amino pyridine (0.18 g, 1.9 mmol) was dissolved in 30 ml acetone and added drop-wise to a stirred acetone solution of **(1)** (0.50 g, 0.96 mmol). The solution was stirred for 2 h and then was evaporated under vacuum, washed with ether to afford an oily product which was dried under vacuum. The compound is soluble in chloroform, dichloromethane, acetonitrile, ethanol and acetone.

[Zn(nap)$_2$(2-ampy)$_2$] **(4)**: (80%) yield, m.p. (74-80) ^{o}C; ^{1}H NMR ($CDCl_3$): δ = 1.52 (d, 3H, CH_3, $^3J_{H-H}$ = 6.9 Hz), 3.86 (q, 1H, CH), 3.88 (s, 3H, OCH_3), 5.71 (bs, 2H, NH_2), 6.23 (t, 1H, CH_{py}, $^3J_{H-H}$ = 6.3 Hz), 7.04 (bs, 1H, CH), 7.07 (d, 1H, CH, $^3J_{H-H}$ = 2.1 Hz), 7.18 (t, 1H, CH_{py}, $^3J_{H-H}$ = 6.9 Hz), 7.42(d, 1H, CH), 7.45 (d, 1H, CH_{Py}), 7.55 (d, 1H, CH, $^3J_{H-H}$ = 7.8 Hz), 7.58 (d, 1H, CH, $^3J_{H-H}$ = 3.9 Hz), 7.59 (d, 1H, CH_{py}, $^3J_{H-H}$ = 5.1 Hz), 7.64 (s, 1H, CH); ^{13}C{^{1}H} NMR ($CDCl_3$): δ = 19.60 (CH_3), 47.53 (**C**H-

CH_3), 55.50 (O-CH_3), 105.75 (CH), 111.36 (CH_{py}), 113.00 (CH_{py}), 118.66 (CH), 125.96 (CH), 126.80 (CH), 127.36 (CH), 129.34 (CH), 139.23 (CH_{py}), 146.17 (CH_{py}), 157. 40 (**C**-OCH_3), 159.19 (C-$NH_{2\ py}$), 181.52 (C=O); IR (cm^{-1}, KBr): 3335, 3211, 3056, 2970, 2933, 1605, 1501, 1452, 1389, 1358, 1267, 1212, 1160, 1120, 1063, 1031, 960, 927, 853, 812, 771, 691, 522, 475, 417; UV-Vis, ($CHCl_3$), λ (nm): 265, 275, 320, 333.

3.3.5 Synthesis of $[Zn(nap)_2(imid)_2]$ (5)

Same procedure was followed as in complex **2** except with imidazole (0.26 g, 3.8 mmol) and complex **(1)** (1.0 g, 1.9 mmol). The compound is soluble in chloroform and DMSO.

$[Zn(nap)_2(imid)_2]$ **(5)**: (78%) yield, m.p. (152-155) ^oC; ^1H NMR (DMSO-d^6): δ = 1.44 (d, 3H, CH_3, $^3J_{H-H}$ = 6.9 Hz), 3.74 (q, 1H, CH, $^3J_{H-H}$ = 6.9 Hz), 3.83 (s, 3H, OCH_3), 7.10 (d, 1H, CH, $^3J_{H-H}$ = 8.4 Hz and 2H, CH_{Imid}), 7.23 (s, 1H, CH), 7.46 (d, 1H, CH, $^3J_{H-H}$ = 8.7 Hz), 7.69 (bs, 2H, 2CH and CH_{Imid}), 7.71 (d, 1H, CH, $^3J_{H-H}$ = 12 Hz), 8.02 (bs, 1H, NH_{Imid}); $^{13}C\{^1H\}$ NMR (DMSO-d^6): δ = 20.36 (CH_3), 47.04 (**C**H-CH_3), 55.76 (O-CH_3), 106.32 (CH), 119.08 (CH), 125.97 (CH), 127.13 (CH), 127.54 (CH), 129.15 (CH), 129.69 (CH_{Imid}), 133.63 (CH), 139.32 (CH_{Imid}), 157.51 (**C**-OCH_3), 178.93 (C=O); IR (cm^{-1}, KBr): 3127, 3055, 2935, 2865, 1608, 1586, 1503, 1452, 1390, 1342, 1265, 1208, 1160, 1072, 1027, 956, 927, 857, 814, 760, 692, 624, 534, 473, 413; UV-Vis, ($CHCl_3$), λ (nm): 264, 274, 320, 334.

3.3.6 Synthesis of $[Zn(nap)_2(1,2\text{-dmimid})_2]$ (6)

Same procedure was followed as in complex 2 except with 1,2-dimethyl imidazole (0.2 ml, 2.3 mmol) and complex **(1)** (0.6 g, 1.15 mmol). The compound is soluble in chloroform, dichloromethane, ethanol and acetonitrile.

$[Zn(nap)_2(1,2\text{-dmimid})_2]$**(6)**: (83%) yield, m.p. (132-136) ^oC; ^1H NMR ($CDCl_3$): δ = 1.50 (d, 3H, CH_3, $^3J_{H-H}$ = 7.2 Hz), 2.01 (s,3H, $CH_{3\ Imid}$), 3.23 (s, 3H, CH_{3Imid}), 3.83 (q, 1H, CH), 3.87 (s, 3H, OCH_3), 6.53 (bs, 1H, CH_{Imid}), 6.83 (bs, 1H, CH_{Imid}), 7.03 (s, 1H, CH), 7.05 (d, 1H, CH, $^3J_{H-H}$ = 2.4 Hz), 7.49 (d, 1H, CH), 7.51 (d, 1H, CH, $^3J_{H-H}$ = 6 Hz), 7.56 (d, 1H, CH, $^3J_{H-H}$ = 9.3 Hz), 7.65 (s, 1H, CH); $^{13}C\{^1H\}$ NMR ($CDCl_3$): δ = 11.70 (CH_{3Imid}), 19.83 (CH_3), 33.21 (N-CH_{3Imid}), 47.83 (**C**H-CH_3), 55.49 (O-CH_3), 105.66 (CH), 118.33 (CH), 120.37 (CH_{Imid}), 125.84 (CH), 126.35 (CH), 127.74 (CH), 129.17 (CH), 129.45 (CH_{Imid}), 133.28 (CH), 146.67 (C_{Imid}), 157.20 (**C**-OCH_3), 180.54 (C=O); IR (cm^{-1}, KBr): 3118, 3056, 2966, 2932, 1605, 1505, 1461, 1418, 1376, 1341, 1265, 1212, 1157, 1119, 1093, 1062, 1029, 958, 926, 854, 824, 776, 747, 674, 652, 553, 479, 445; UV-Vis, ($CHCl_3$), λ (nm): 264, 274, 320, 335.

3.4 X-ray crystallography

X-ray intensities data of complex **3** was carried out at room temperature on a Bruker SMART APEX CCD X-ray diffractometer system (graphite–monochromated Mo Kα radiation λ = 0.71073 Å) by using the SMART software package [71]. The data were reduced and integrated by the SAINT program package [72]. The structure was solved

and refined by the SHELXTL software package [73]. H atoms were located geometrically and treated with a riding model. Crystal data and details of the data collection and refinement are summarized in Table 5.

Table 5

Crystal data and structure refinement for [Zn(nap)$_2$2,9-dimethyl-1,10-phenanthroline] **(3)**

Empirical formula	$C_{44}\ H_{41}N_3\ O_6\ Zn$	
Formula weight	773.17	
Temperature	173(1) K	
Wavelength	0.71073 Å	
Crystal system	Monoclinic	
Space group	P2(1)	
Unit cell dimensions	a = 15.0063(9) Å	α = 90°.
	b = 14.1711(8) Å	β = 91.705(1)°.
	c = 17.796(1) Å	γ = 90°.
Volume	3782.7(4) Å^3	
Z	4	
Density (calculated)	1.358 Mg/m^3	
Absorption coefficient	0.703 mm^{-1}	
F(000)	1616	
Crystal size	0.28 x 0.24 x 0.17 mm^3	
Theta range for data collection	2.26 to 27.00°.	
Index ranges	-18<=h<=19, -18<=k<=18, -22<=l<=22	
Reflections collected	31490	
Independent reflections	16184 [R(int) = 0.0398]	
Completeness to theta = 27.00°	99.8 %	
Absorption correction	None	
Refinement method	Full-matrix least-squares on F^2	
Data / restraints / parameters	16184 / 1 / 963	
Goodness-of-fit on F^2	0.993	
Final R indices [I>2sigma(I)]	R1 = 0.0698, wR2 = 0.1714	
R indices (all data)	R1 = 0.0978, wR2 = 0.1878	
Absolute structure parameter	0.043(13)	
Largest diff. peak and hole	1.132 and -0.647 e.Å^{-3}	

a $R1 = \sum ||Fo| - |Fc|| / \sum Fo$ and $wR2 = \{\sum[w(F02 - Fc2)2] / \sum[w(Fo2)2]\}1/2$

3.5 Anti-bacterial activity

Zn(II) naproxen complexes **(1-6)** were screened for their anti-bacterial activity against G^+-bacteria (*Staphylococcus aureus* and *Micrococcus luteus)* and G^--bacteria *(Klebsiella pneumoniae, Proteus mirabilis, Pseudomonas aeruginosa* and *Escherichia coli).* These complexes were tested *in vitro* using the agar well diffusion method [74]. Single bacteria colonies were dissolved in sterile saline to obtain suspended cells with turbidity equivalent to a MC Farland 0.5 standard. The bacterial inocula were spreed on the surface of the nutrient agar with the help of a sterile cotton swab, then 6 mm diameters wells were dug in agar medium using sterile glassy borer.

The Zinc(II) complexes were prepared in DMSO (8.5 mmol/L) and were introduced into the respective wells using 50 *μL* pipette, one of the wells was supplemented with DMSO as control. These plates were placed in a 37 ^oC incubator for 24 h to allow bacterial growth. After 24 h, the diameter of the inhibition zone (in mm) was measured.

The minimum inhibitory concentration (MIC) was determined for each complex (only complexes **2**, **3** and **4** and there parent ligands because of their significant preliminary results) as the lowest concentration which was capable of stopping bacterial growth. Sequential dilutions of these complexes and their parent ligands in DMSO in the range 8.5 mmol/L to 0.265 mmol/L, were prepared to determine the MIC using the same previous procedure. When inhibition was present, the clear zone around the well for each complex was compared with its parent ligands in the same plate and the diameter of the inhibition zone was measured.

3.6 Anti-malarial activity

3.6.1 *In vitro* testing for anti-malarial activity using Semi-Quantitative method

The procedure for in vitro testing was carried out according to Deharo et.al [19]. A mixture containing 50 μL of (0.5 mg/ml) hemin chloride freshly dissolved in (DMSO), 100 μL of (0.5 M) sodium acetate buffer (pH 4.4), and 50 μL of different concentrations of the complex dissolved in pure water, was incubated in a normal non-sterile 96-well flat bottom plate at 37 ºC for 18-24 h. It is important that the solutions be added to the plate in this order. The plate was then centrifuged for 10 min at 4000 rpm. The supernatant was removed and the pH of reaction was measured. The final pH of the mixture should be between (5.0-5.2). The wells were washed with 200 μL DMSO per well to remove free hemin chloride. The plate was centrifuged again, discarding the supernatant afterwards. The residual β -hematin was then dissolved in 200 μL of 0.1 M NaOH to form an FP that can be measured spectrophotometrically. Finally, the absorbance was measured at 405 nm using ELISA reader Note, ultra pure water was used as negative control; meanwhile chloroquine dissolved in ultra-pure water was used as positive control.

3.6.2 Quantitative test

The method of Blauer and Akkawi was adopted for quantitative test [21]. Freshly prepared stock solution of hemin chloride was prepared by dissolving the salt in (DMSO) and incubated for 30 min at 30°C stock solution of the complex used was

prepared using DMSO (0.5 M) sodium acetate buffer (pH 4.4) was also prepared, the final concentration of hemin and the complex in the reaction were 0.2 and 0.4 mM respectively, the whole mixture was left for 18-24 hrs at 37℃ without stirring. The total volume of the reaction mixture was 32 mL, and the final pH was 4.9 to 5.2.

Samples were centrifuged for 10 min using a serological (Jouan B4) centrifuge. The supernatant was discarded and the precipitate was washed with DMSO and quantitatively transferred to a Millipore Swinnex 13 filter containing Whatman filter paper No. 50, already lyophilized to a constant weight in freeze-drying machine (Labconco Freezone). DMSO was passed slowly through the filter until the filtrate remained feebly colored and washed again with ultra-pure water. The remaining was then lyophilized to a constant weight.

4. Conclusion

Six zinc naproxen complexes were prepared and fully characterized by IR, UV-Vis, ^{1}H NMR, ^{13}C{^{1}H} NMR spectroscopy. X-ray crystal structure for complex **3** was also determined.

These complexes exhibit variant anti-bacterial activity against the tested bacterial species. Complex **2** showed lower anti-bacterial activity against all available bacterial species when compared to 1,10-phenanthroline ligand. Complex **2** was the only complex that showed anti-bacterial activity against *P. aeruginosa*, which may be due to the complexation of the active 1,10-phenathroline parent ligand. Complex **3** showed higher anti-bacterial activity against G^- bacteria compared to 2,9-dimethyl-1,10-phenanthroline ligand, but this ligand showed higher anti-bacterial activity against G^+ than complex **3**.

Complex **3** showed very high inhibition activity on the formation of the β-hematin and it has the potential to be further developed as an effective anti-malarial drug.

Acknowledgment

The authors thank the office of Vice President for Academic Affairs at Birzeit University for their financial support.

Appendix A. Supplementary material

CCDC1006594 (3) contain the supplementary crystallographic data for this paper. These data can be obtained free of charge from the Cambridge Crystallographic Data Centre via www.ccdc.cam.ac.uk/data_request/cif.
Supplementary data to this article can be found online at http://xxxxxx

References

[1] K. Gyoryova; E. Szunyogova; J. Kovarova; D. Hudecova; D. Mudronova; E. Juhaszova. J. Therm. Anal. Calorim. 72 (2003) 587-596.

[2] L. Bertini; C. Luchinat; R. Monnanni; J. Chem. Edu. 62 **(**1985) 924-927.

[3] B. L. Vallee; D. S. Auld. Biochemistry. 29 (1990) 5647-5659.

[4] H. Tapiero; K. D. Tew. Biomedicine and Pharmacotherapy. 57 (2003) 399-411.

[5] Y. Yunhua; D. Guangjian; T. Shaozao; L. Yingliang; S. Qingshan; O. Yousheng. J. Rare. Earths. 29 *(*2011) 308-312.

[6] Z. Bujdosova; K. Gyoryova; J. Kovarova; D. Hudecova; L. Halas. J. Therm, Anal. Calorim. 98 (2009) 151-159.

[7] E. Andogova; k. Gyoryova; Nour F. A. el-dien. J. Therm. Anal. Calorim. 69 (2002) 245-253.

[8] Z. H. Chohan; M. A. Farooq. Pakistan J. Pharm. Sci. 7 (1994) 45-53.

[9] E. L. Chang; C. Simmers; D. A. Knight. Pharmaceuticals. 3 (2010) 1711-1728.

[10] B. S. Sekhon; N. Bimal. J. Pharm. Educ. Res. 3 (2012) 52-63.

[11] M. E. Drew; R. Banerjee; E. W. Uffman; S. Gilbertson; P. J. Rosenthal; D. E. Goldberg. J. Biol. Chem. 283 (2008) 12870-12876.

[12] D. E. Goldberg. Curr. Top. Microbiol. Immunol. 295 (2005) 275-291.

[13] P. Dzomba; T. Chayamiti; S. Nyoni; P. Munosiyei; I. Gwizangwe. Afr. J. Pharm. Pharmacol. 6 (2012) 2205-2210.

[14] S. Pagola; P.W. Stephens, D.S. Bohle, A.D. Kosar and S.K. Madsen. Nature. 404 (2000) 307-310.

[15] R. Lemberg; J. W. Legge. Interscience. NewYork, (1949).

[16] J. Ziegler; R. Linck; D.W. Wright. Curr Med Chem, 8 (2001) 171-189.

[17] E. W. Thomas and V. P. Christopher. J Infect Dis. 184 (2001) 770-776.

[18] L. W. Karena, A. M. Rebecca, M. U. Lyann, H. Paul, V. Dominik, B. S. Amar, F. Hisashi, D. R. Paul, David A. F. J. Biol. Chem. 278 (2003) 33593-33601.

[19] E. Deharo; R. N. Garcia; P. Oporto; A. Gimenez; M. Sauvian; V. Jullian; H. Ginsburg. Exp. Parasitol. 100 (2002) 252-256.

[20] G. Blauer; M. Akkawi. Arch. Biochem. Biophys. 398 (2002) 7-11.

[21] G. Blauer; M. Akkawi. J. Inorg. Biochem. 66 (1997) 145-152.

[22] F. Dimiza; F. Perdih; V. Tangoulis; T. Turel; D.P. Kessissoglou; G. Psomas. J. Inorg. Biochem. 105 (2011) 476-489.

[23] R. Dua; S. Shrivastava; S. K. Sonwane; S. K. Srivastava. Advan. Biol. Res. 5 (2011) 120-144.

[24] J. Sharma; A.K. Singla; S. Dhawan. Int. J. Pharm. 260 (2003) 217-227.

[25] S. Q. Field. Why theses antifreeze in your toothpaste: the chemistry of household ingredients, 1st ed.; Chicago review press: (2007) 184.

[26] S. Yaqub; I. Ul-Haq; .S Ali; B. Mirza; F. Ahmed; S. Shahzadi. J. Coord. Chem. 62 (2009) 3463-3470.

[27] K. Gyoryova; J. Kovarova; E. Anogova,; V. Zelenak,; F.A. Nour el-dien. J. Therm. Anal. Calorim. 67 (2002) 119-128.

[28] K. Gyoryova; V. Balek; V. Zelenak. Thermochimicaacta. 234 (1994) 221-232.

[29] K. Gyoryova; M. Melnik; E. Andogova. J. Therm. Anal. Calorim. 56 (1999) 503.

[30] K. Gyoryova; J. Chomic; E. Szunyogova; L. Piknova; V. Zelenak; Z. Vogarova. J. Therm. Anal. Calorim. 84 (2006) 727-732.

[31] K. Gyoryova; J. Chomic; J.Kovarova. J. Therm. Anal. Calorim. 80 (2005) 375-380.

[32] J. Chomic; K. Gyoryova; E. Szunyogova; J. Kovarova. J. Therm. Anal. Calorim. 76 (2004) 33-41.

[33] Y. Wang; M. Odoko; N. Okabe. ActaCryst. C60 **(**2004) m 479.

[34] L. Findorakova; K. Gyoryova; J. Kovarova; V. Balek; F.A. Nour el-dien; L. Halas. J. Therm. Anal. Calorim. 95 (2009) 923-928.

[35] V. Zelenak; K. Gyoryova; M. Ceckova. ThermochimaActa. 371 (2001) 103-109.

[36] V. Zelenak; K. Gyoryova; E. Andogova. ThermochimaActa. 354 (2000) 81-88.

[37] A. Krajnikova; K. Gyoryova; D. Hudecova; J. Kovarova; Z. Vargova. J. Therm. Anal. Calorim. 105 (2010) 451-460.

[38] K. Gyoryova; V. Balek. J. Therm. Anal. Calorim. 40 (1993) 519-532.

[39] F. Dimiza; A. N. Papadopoulos; V. Tangoulis; V. Psycharis; C. P. Raptopoulou; D. P. Kessissoglou; G. Psomas; J. Inorg. Biochem. 107 (2012) 54-64.

[40] H. M. Butler; A. Hurse; E. Thursky; A. Shulman. Aust. J. exp. Biol, Med, Sci. 47 (1969) 541-552.

[41] M. O. Agwara; P. T. Ndifon; N. B. Ndosiri; A.G. Paboudam; D. M. Yufanyi; A. Mohamadou. Bull. Chem. Soc. Ethiop. 24 (2010) 383-389.

[42] J. Salimon; N. Salih; H. Hussien; E. Yousif. Europ. J. Sci. Res. 31 (2009) 256-264.

[43] M. F.V. Moura; O. A. Oliveira; R. Farias. Thrmochemica Acta. 405 (2003) 219-224.

[44] S. Ur-rehman; M. Ikram; S. Rehman; A. Faiz; Shahnawaz. Bull. Chem. Soc. Ethiop. 24 (2010) 201-207.

[45] F. P. Dwyer; I. K. Reid. Aust. J. Exp. Biol. Med. Sci. 47 (1969**)** 203-218.

[46] M. N. Patel; P. A. Parmer; D. S. Gandhi; V. R.Thakkar. J. Enzyme Inhib. Med. Chem. 26 (2011) 359-366.

[47] A. Shulman; D. O. White. Chem.-Biol. Interact. 6 (1973) 407-413.

[48] D. O. White; A. W. Harris. Aust. J. Exp. Biol. 41 (1963) 517-526.

[49] F. Dumitrascu; M. R. Caira; C. Draghici; M. T. Caproiu; L. Barbu; B. Miu. Rev. Roum. Chim. 53 (2008) 183-187.

[50] C. H. Chang; J. W. Yarbro; D. E. Mann; R. F. Gautieri. J. Pharmacol. Exp. Ther. 205 (1978) 27-32.

[51] R. N. Patel; N. Singh; K. K. Shukla; U. K. Chauhan; J. Niclos-Gutierrez; A. Castineiras. Inorg. Chem. Acta. 357 (2004) 2469-2476.

[52] A. Mohindru; J. M. Fisher; M. Rabinovitz. Biochem. Pharmacol. 32 (1983) 3627-3632.

[53] A. Shulman; G. M. Laycock. Chem. Biol. Interact. 16 (1977) 89-99.

[54] V. Zelenak; I. Cisarova; M. Sapo; P. Lewellyn; K. Gyoryova. J. Coord. Chem. 57 (2004) 87.

[55] K. L. Zhang; J. G. Lin; Y. Q. Wang; W. L. Xu; J. T. Chen. Acta Cryst. C60 (2004) m454-m456.

[56] Y. Zheng; Q. Yang; Xu. D. Jun. Acta Cryst. E62 (2006) m 813-m815.

[57] A.W. Addison, T. Nageswara Rao, J. Reedijk, J. van Rijn, G.C. Verschoor. J. Chem. Soc., Dalton Trans., (1984) 1349-1356.

[58] S. B. Etcheverry; D. A. Barrio; A. M. Cortizo; P. A. M. Williams. J. Inorg. Biochem. 88 (2002) 94-100.
[59] K. Kafarska; D. Czakis-Sulikowska; W. M. Wolf. J. Therm. Anal. Calorim. 96 (2009) 617-621.
[60] Z. N Chen; R. W Deng; J. G. Wu. J. Inorg. Biochem. 47 (1992) 81-87.

[61] A. Abuhijleh; J. Khalaf. Europ. J. Med. Chem. 45 (2010) 3811-3817.
[62] G.B. Deacon, R.J. Philips, Coord. Chem. Rev. 33 (1980) 227-250.

[63] V. Zelenak, Z. Vargova, K. Gyoryova, Spectrochim. Acta Part A 66 (2007) 262-272.

[64] X. M. Chen; B. H.Ye,; X. C. Huang; Z. T. Xu. J. Chem.Soc. Dalton Trans. (1996) 3465.
[65] A. Tarushi; G. Psomas; C. P. Raptopoulou; D. P. Kessissoglou. J. Inorg. Biochem. 103 (2009) 898-905.

[66] F. Yilmaz; V. T. Yilmaz; E. Bicer; O. Z. Buyukgungor. Naturforsch. 61b (2006) 275-280.
[67] S. A. Shaker; Y. Farina. Am. J. sci. res. issue 5 (2009) 20.
[68] Spectral Database for organic compounds (SDBS)- RIO-DB-AIST.

[69] K. Nakamoto. *Infrared and Raman spectra of inorganic and coordination compounds. Part B: Applications in coordination, organometallic and bioinorganic chemistry*, 6th ed.; John Wiley and sons, Inc., publication. 2009.
[70] I. Weissbuch; L. Leiserowitz. Chem. Rev. 108 (2008) 4899-4914.

[71] SMART-NT V5.6, Bruker AXS GMBH, D-76181 Karlsruhe, Germany, 2002.

[72] SAINT-NT V5.0, BRUKER AXS GMBH, D-76181 Karlsruhe, Germany, 2002.

[73] SHELXTL-NT V6.1, BRUKER AXS GMBH, D-76181 Karlsruhe, Germany, 2002.

[74] M.I. Atta-ur-Rahman, Choudhary W.J. Thomson, Bioassay Techniques for Drug Development, Harwood Academic, The Netherlands, 2001.

Highlights:

► New mixed ligand zinc(II) complexes of naproxen acid and nitrogen-based ligands were synthesized
►The complexes were characterized using various spectrometric techniques.
► In-vitro anti-bacterial activity against several bacterial species was studied.
► In-vitro anti-malarial activity of complex **3** against the formation of β-Hematin was determined.

Supporting information

Table S1: Physical properties of zinc naproxen complexes **1-6**.

Complex	Yeild %	M.p.(˚C)	Solubility
$[Zn_2(nap)_4]$ **(1)**	86	228-233	Acetone, acetonitrile, dichloromethane, methanol, ethanol.
$[Zn(nap)_2$1,10-Phen] **(2)**	80	220-230	Dichloromethane, methanol.
$[Zn(nap)_2$2,9-dmphen] **(3)**	72	209-213	Chloroform, acetonitrile, acetone.
$[Zn(nap)_2(2\text{-ampy})_2]$ **(4)**	80	74-80	Ethanol, acetone, acetonitrile, dichloromethane, chloroform.
$[Zn(nap)_2(imid)_2]$ **(5)**	78	152-155	Chloroform , DMSO.
$[Zn(nap)_2(1,2\text{-dmimid})_2]$ **(6)**	83	132-136	Ethanol, chloroform, acetonitrile ,dichloromethane.

Table S2

Selected bond distances (Å) and bond angles (°) for **3.**

Bond distance (Å)			
Zn(1)-N(1)	2.100	Zn(2)-O(10)	1.921
Zn(1)-N(2)	2.045	Zn(2)-O(11)	2.997[a]
Zn(1)-O(1)	1.960	C(15)-O(1)	1.233
Zn(1)-O(2)	2.927[a]	C(15)-O(2)	1.250
Zn(1)-O(4)	1.979	C(29)-O(4)	1.250
Zn(1)-O(5)	2.792[a]	C(29)-O(5)	1.191
Zn(2)-N(3)	2.086	C(57)-O(7)	1.243
Zn(2)-N(4)	2.072	C(57)-O(8)	1.216
Zn(2)-O(7)	2.241	C(71)-O(10)	1.307
Zn(2)-O(8)	2.141	C(71)-O(11)	1.226
Bond angle (°)			
N(1)-Zn(1)-N(2)	80.82	N(3)-Zn(2)-O(8)	91.39
N(1)-Zn(1)-O(1)	119.29	N(3)-Zn(2)-O(7)	137.59
N(1)-Zn(1)-O(4)	101.91	N(4)-Zn(2)-O(7)	97.05
N(2)-Zn(1)-O(1)	119.83	N(4)-Zn(2)-O(8)	130.98
N(2)-Zn(1)-O(4)	131.54	N(4)-Zn(2)-O(10)	124.74
O(1)-Zn(1)-O(4)	101.11	O(7)-Zn(2)-O(8)	58.24
N(3)-Zn(2)-N(4)	80.61	O(7)-Zn(2)-O(10)	99.96
N(3)-Zn(2)-O(10)	116.29	O(8)-Zn(2)-O(10)	102.25

a: Non-bonded contact distance

Table S3: IR data of complex **1** and Na(nap) in (cm^{-1}).

Assignments	Na(nap)	$[Zn_2(nap)_4]$ (1)
$\upsilon(C\text{-}H)_{ar}$	3070	3080
$\upsilon(C\text{-}H)_{aliph}$	2959	2955
$\upsilon_{as}(COO^-)$	1540	1600
$\upsilon_s(COO^-)$	1385	1390
υ(ring) + δ(C-H)	1625,1480,1440,1360,1207,1160,1028	1630,1485,1455,1370,1210,1160,1027
υ(C-O)	1260	1260
$\Delta\upsilon(COO^-)$	155	210

Table S4: IR data of complexes **2-4** in (cm^{-1}).

Assignments	2	3	4
υ_{as}(N-H)	-	-	3335
$_s$ (N-H)υ	-	-	3211
$\upsilon(C\text{-}H)_{ar}$	3056	3056	3057
υ $(C\text{-}H)_{aliph}$	2969,2931	2964,2930	2970,2933
$\upsilon_{as}(COO^-)$	1603	1605	1605
υ(ring) + δ(C-H)	1522,1483	1505,1453	1501,1452
	1458		
$\upsilon_s(COO^-)$	1388	1375	1389
$\upsilon(C\text{-}NH_2)$	-	-	1358
υ(C-O)	1262	1267	1267
υ(ring)	1211,1159	1212,1156	1212,1160
	1121,1061	1121,1033	1120,1063
	1029		1031
γ(C-H)	853,824	852,813	853,771
$\Delta\upsilon(COO^-)$	215	230	216

Table S5: Selected IR results of complexes **5** and **6** in (cm^{-1}).

Assignments	5	6
(N-H)υ	3127	-
$\upsilon(C\text{-}H)_{ar}$	3055	3056
$\upsilon\ (C\text{-}H)_{aliph}$	2935,2865	2966,2932
$\upsilon_{as}(COO^-)$	1608	1605
υ(ring) + δ(C-H)	1608,1503,1586	1605,1505,1461
	1452	1418
$\upsilon_s(COO^-)$	1390	1376
υ(C-N)	1342	1341
υ(C-O)	1265	1264
υ(ring)	1208,1160	1212,1157
	1072,1027	1119,1062
		1029
γ(C-H)	857,814,760	853,824,747
$\Delta\upsilon(COO^-)$	196	229

Table S6: ^{1}H and $^{13}C\{^{1}H\}$ NMR data for complex **1** and naproxen.

^{1}H NMR for $[Zn_2(nap)_4]$(1)		**^{1}H NMR for (nap)**	**$^{13}C\{^{1}H\}$ NMR for $[Zn_2(nap)_4]$ (1)**		**$^{13}C\{^{1}H\}$ for NMR(nap)**
(d, 3H, CH_3)	1.39	1.57	(CH_3)	19.59	19.07
(bs, 1H, **CH**-CH_3)	3.70	3.86	(**C**H-CH_3)	48.37	45.91
(s, 3H, OCH_3)	3.90	3.87	(O-CH_3)	55.44	55.26
(bs, 1H, CH)	7.00	7.08	(CH)	105.70	105.4
(d, 1H, CH, ^{3}J= 8.4Hz)	7.08	7.12	(CH)	118.82	118.60
(bs, 1H, CH)	7.42	7.40	(CH)	125.88	126.0
(s, 1H, CH)	7.54	7.66	(CH)	126.87	126.18
(d, 1H, CH)	7.58	7.67	(CH)	127.17	127.1
(d, 1H, CH)	7.61	7.67	(CH)	129.26	128.86
		(COOH) 12.34	(CH)	133.51	133.0
			(**C**-OCH_3)	157.44	156.1
			(C=O)	181.41	180.0

Table S7: ^{1}H and $^{13}C\{^{1}H\}$ NMR data for complex **2** and 1,10-phen.

^{1}H NMR for (2)	**^{1}H NMR for 1,10-phenanthroline**	**$^{13}C\{^{1}H\}$ NMR for (2)**	**$^{13}C\{^{1}H\}$ NMR for Phenanthroline1,10-**
(d, 3H, CH_3, $^{3}J_{H-H}$ = 6.9Hz) 1.52		(CH_3) 19.58	
(bs, 4H, CH, OCH_3) 3.87		(**C**H-CH_3) 46.67	
(d, 1H, CH, $^{3}J_{H-H}$ = 3Hz) 7.02		(O-CH_3) 55.49	
(d, 1H, CH, $^{3}J_{H-H}$ = 1.5 Hz) 7.06		(CH) 105.69	
(d, 2H, CH, $^{3}J_{H-H}$ = 8.1 Hz) 7.40		(CH) 118.59	
(d, 1H, CH, $^{3}J_{H-H}$ = 8.7 Hz) 7.49		($2CH_{Phen}$) 120.96	122.90
(d, 2H, 2CH) 7.52		(CH) 125.86	
(bs, 2H, CH_{Phen}) 7.60	8.20	(CH) 126.74	
(t,2H,CH_{Phen}, $^{3}J_{H-H}$ = 7.8 Hz) 7.68	7.58	(CH) 127.34	
(bs, 2H, CH_{Phen}) 7.81	8.22	(CH) 129.12	
(d, 2H, CH_{Phen}) 8.53	9.18	($2CH_{Phen}$) 129.44	128.46
		(CH) 133.48	
		($2CH_{Phen}$) 138.68	135.81
		($2CH_{Phen}$) 139.91	146.10
		($2CH_{Phen}$) 149.64	150.12
		(**C**-OCH_3) 157.38	

Table S8: ^{1}H and $^{13}C\{^{1}H\}$ NMR data for complex **3** and 2,9-dmphen.

^{1}H NMR for (3)		**^{1}H NMR for 2,9-dimethyl-1,10-phenanthroline**	**$^{13}C\{^{1}H\}$ NMR for (3)**		**$^{13}C\{^{1}H\}$ NMR for 2,9-dimethyl-1,10 Phenanthroline**
(d, 3H, CH_3, $^{3}J_{H-H}$ = 7.2 Hz)	1.49		(CH_3)	19.75	
(s, 6H, CH_{3Phen})	2.74	2.92	($2CH_{3Phen}$)	24.81	25.79
(q, 1H, CH)	3.86		(**C**H-CH_3)	47.06	
(s, 3H, OCH_3)	3.89		(O-CH_3)	55.48	
(bs, 1H, CH)	7.03		(CH)	105.70	
(d, 1H, CH, $^{3}J_{H-H}$ = 2.7 Hz)	7.06		(CH)	118.49	
(d, 2H, CH_{Phen}, $^{3}J_{H-H}$ = 2.7 Hz)	7.40	7.46	($2CH_{Phen}$)	125.70	123.44
(d, 1H, CH)	7.43		(CH)	125.81	
(d, 2H, CH_{nap}, $^{3}J_{H-H}$ = 8.7 Hz)	7.51		($2CH_{Phen}$)	126.36	125.40
(bs, 1H, CH)	7.59		(CH)	126.61	
(d, 2H, CH_{Phen}, $^{3}J_{H-H}$ = 3.9 Hz)	7.69	7.69	(CH)	127.12	
(d, 2H, CH_{Phen}, $^{3}J_{H-H}$ = 8.4 Hz)	8.17	8.10	($2C_{phen}$)	127.39	126.78
			(CH)	129.29	
			($2CH_{Phen}$)	132.12	136.23
			(CH)	133.40	
			($2CH_{Phen}$)	139.11	145.27
			(**C**-OCH_3)	157.29	
			($2CH_{Phen}$)	160.76	159.23
			(C=O)	181.87	

Table S9: ^{1}H and $^{13}C\{^{1}H\}$ NMR data for complex **4** and 2-ampy.

^{1}H NMR for (4)		**^{1}H NMR for 2-amino pyridine**	**$^{13}C\{^{1}H\}$ NMR for (4)**		**$^{13}C\{^{1}H\}$ NMR for 2-amino pyridine**
(d, 3H, CH_3, $^{3}J_{H-H}$ = 6.9 Hz)	1.52		(CH_3)	19.60	
(q, 1H, CH)	3.86		(**C**H-CH_3)	47.53	
(s, 3H, OCH_3)	3.88		(O-CH_3)	55.50	
(bs, 2H, NH_2)	5.71	4.63	(CH)	105.75	
(t, 1H, CH_{pyr}, $^{3}J_{H-H}$ = 6.3 Hz)	6.23	6.47	(CH_{pyr})	111.36	108.66
(bs, 1H, CH)	7.04		(CH_{pyr})	113.00	113.67
(d, 1H, CH, $^{3}J_{H-H}$ = 2.1 Hz)	7.07		(CH)	118.66	
(t, 1H, CH_{pyr}, $^{3}J_{H-H}$ = 6.9 Hz)	7.18	6.60	(CH)	125.96	
(d, 1H, CH)	7.42		(CH)	126.80	
(d, 1H, CH_{Pyr})	7.45	7.38	(CH)	127.36	
(d, 1H, CH, $^{3}J_{H-H}$ = 7.8 Hz)	7.55		(CH)	129.34	
(d, 1H, CH, $^{3}J_{H-H}$ = 3.9 Hz)	7.58		(CH_{pyr})	139.23	137.66
(d, 1H, CH_{pyr}, $^{3}J_{H-H}$ = 5.1 H)	7.59	8.05	(CH_{pyr})	146.17	147.98
(s, 1H, CH)	7.64		(**C**-OCH_3)	157.40	
			(C-$NH_{2\ pyr}$)	159.19	158.85
			(C=O)	181.52	

Table S10: ^{1}H and ^{13}C{^{1}H} NMR data for complex **5** and imid.

^{1}H NMR for (5)		**^{1} H NMR for imidazole**	**^{13}C{^{1}H} NMR for (5)**	**^{13}C{^{1}H} NMR for imidazole**
(d, 3H, CH_3, $^{3}J_{H-H}$ = 6.9Hz)	1.44		(CH_3) 20.36	
(q, 1H, CH, $^{3}J_{H-H}$ = 6.9 Hz)	3.74		(**C**H-CH_3) 47.04	
(s, 3H, OCH_3)	3.83		(O-CH_3) 55.76	
(d, 1H, CH, $^{3}J_{H-H}$ = 8.4 Hz and 2H, CH_{Imid})	7.10	7.13	(CH) 106.32	
(s, 1H, CH)	7.23		(CH) 119.08	
(d, 1H, CH, $^{3}J_{H-H}$ = 8.7 Hz)	7.46		(CH) 125.97	
(bs, 2H, 2CH and CH_{Imid})	7.69		(CH) 127.13	
(d, 1H, CH, $^{3}J_{H-H}$ = 12 Hz)	7.71		(CH) 127.54	
(bs, 1H, NH_{Imid})	8.02	7.73	(CH) 129.15	
			(CH_{Imid}) 129.69	121.88
			(CH) 133.63	
			(CH_{Imid}) 139.32	135.35
			(**C**-OCH_3)157.51	
			(C=O) 178.93	

Table S11:^{1}H and ^{13}C{^{1}H} NMR data for complex **6** and 1,2-dmimid.

^{1}H NMR for (6)		**^{1} H NMR for imidazole**	**^{13}C{^{1}H} NMR for (6)**	**^{13}C{^{1}H} NMR for imidazole**
(d, 3H, CH_3, $^{3}J_{H-H}$ = 6.9Hz)	1.44		(CH_3) 20.36	
(q, 1H, CH, $^{3}J_{H-H}$ = 6.9 Hz)	3.74		(**C**H-CH_3) 47.04	
(s, 3H, OCH_3)	3.83		(O-CH_3) 55.76	
(d, 1H, CH, $^{3}J_{H-H}$ = 8.4 Hz and 2H, CH_{Imid})	7.10	7.13	(CH) 106.32	
(s, 1H, CH)	7.23		(CH) 119.08	
(d, 1H, CH, $^{3}J_{H-H}$ = 8.7 Hz)	7.46		(CH) 125.97	
(bs, 2H, 2CH and CH_{Imid})	7.69		(CH) 127.13	
(d, 1H, CH, $^{3}J_{H-H}$ = 12 Hz)	7.71		(CH) 127.54	
(bs, 1H, NH_{Imid})	8.02	7.73	(CH) 129.15	
			(CH_{Imid}) 129.69	121.88
			(CH) 133.63	
			(CH_{Imid}) 139.32	135.35
			(**C**-OCH_3)157.51	
			(C=O) 178.93	